Supplementary Information

High-performance flexible resistive random access memory devices based on graphene oxidized with a perpendicular oxidation gradient

Tariq Aziz[1,2#], Shi-Jing Wei[1,2,3#], Yun Sun[1,4#], Lai-Peng Ma[1,4*], Song-Feng Pei[1,4], Shichao Dong[1,4], Wen-Cai Ren[1,4], Qi Liu[5*], Hui-Ming Cheng[1,4,6] and Dong-Ming Sun[1,4*]

[1]*Shenyang National Laboratory for Materials Science, Institute of Metal Research, Chinese Academy of Sciences, 72 Wenhua Road, Shenyang, 110016, P. R. China.*

[2]*University of Chinese Academy of Sciences, 19A Yuquan Road, Beijing, 100049, P. R. China.*

[3]*Key Laboratory of Photovoltaic Materials, Henan University, 1 Jinming Road, Kaifeng, 475004, P. R. China.*

[4]*School of Material Science and Engineering, University of Science and Technology of China, 72 Wenhua Road, Shenyang, 110016, P. R. China.*

[5]*Frontier Institute of Chip and System, Fudan University, 2005 Shonghu Road, Shanghai 200433, P. R. China.*

[6]*Tsinghua-Berkeley Shenzhen Institute, Tsinghua University, 1001 Xueyuan Road, Shenzhen, 518055, P. R. China.*

Corresponding authors: Lai-Peng Ma (lpma@imr.ac.cn); Qi Liu (qi_liu@fudan.edu.cn); Dong-Ming Sun (dmsun@imr.ac.cn).

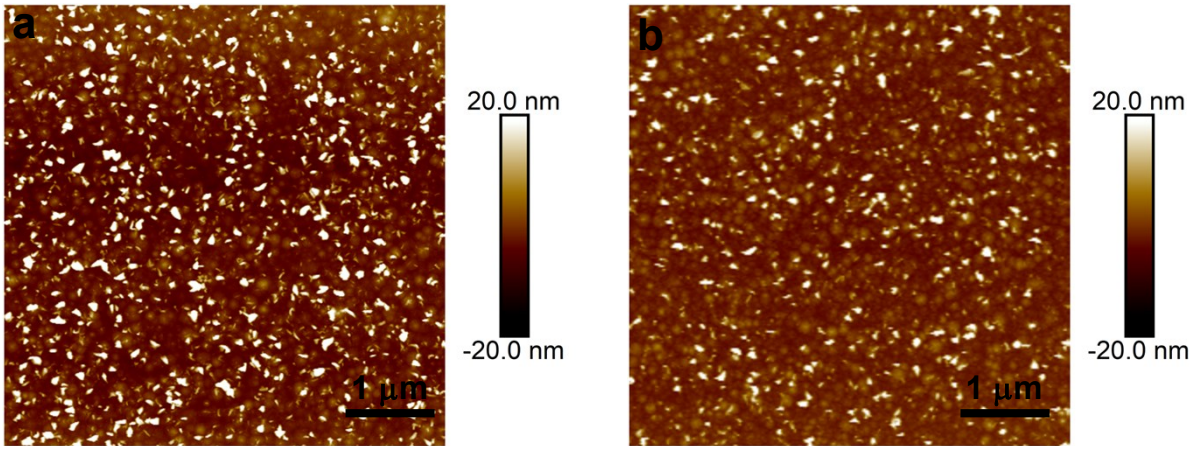

Supplementary Figure 1. Atomic force microscope images of the graphene films. Surface morphology of (a) pristine graphene and (b) POG-graphene.

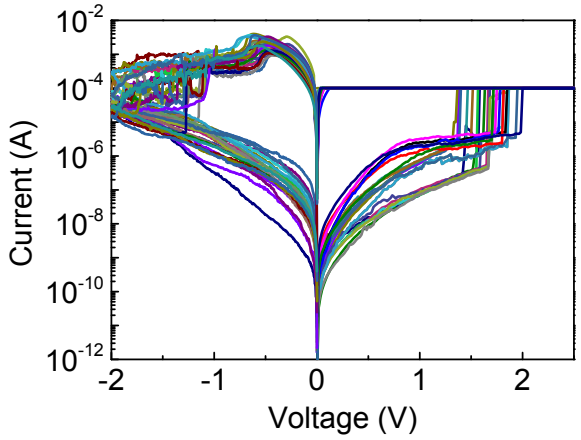

Supplementary Figure 2. *I-V* characteristics of 25 POG-graphene RRAMs indicate the gradual reset process.

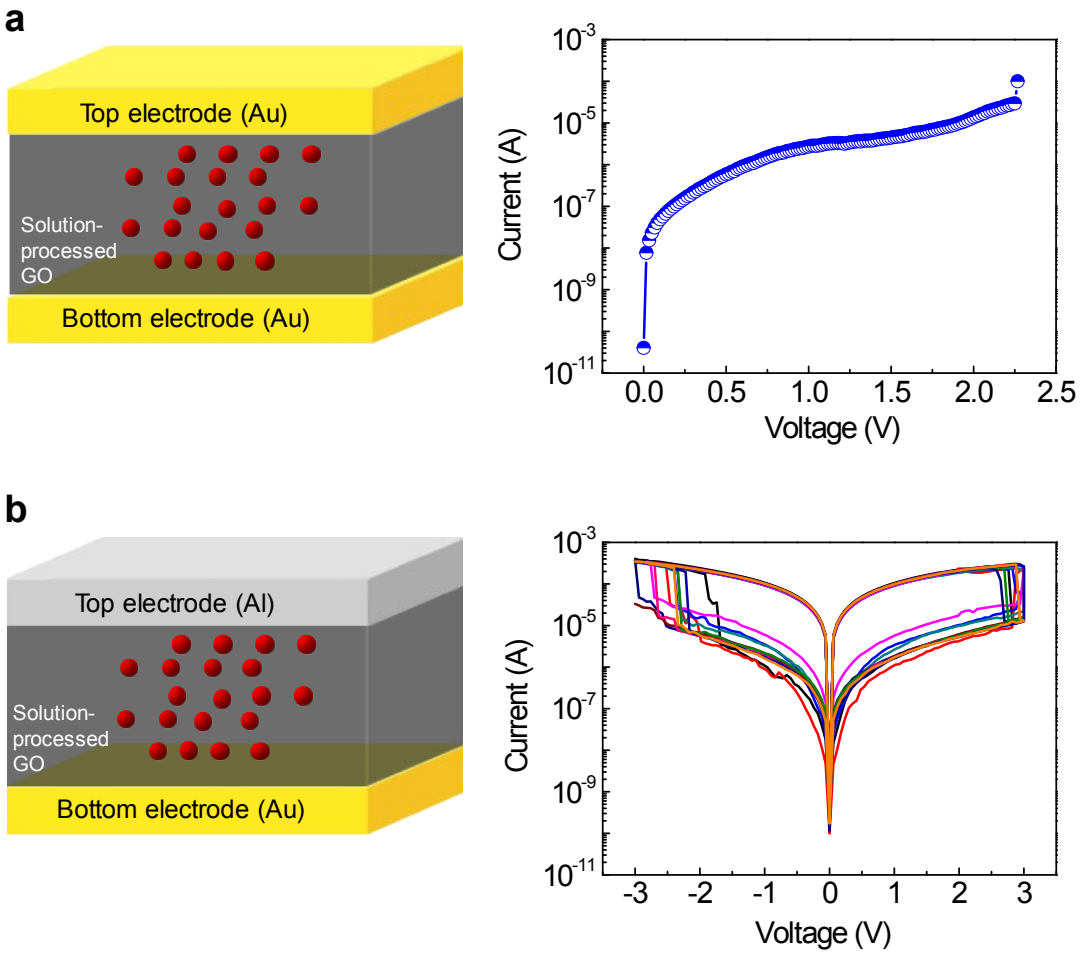

Supplementary Figure 3. Effect of metal electrodes on RRAMs based on solution-processed graphene oxide (GO). Schematic of RRAMs with solution-processed GO as the resistive layer with (a) two Au electrodes without memory performance and (b) Al as the top electrode and Au as the bottom electrode with good memory performance.

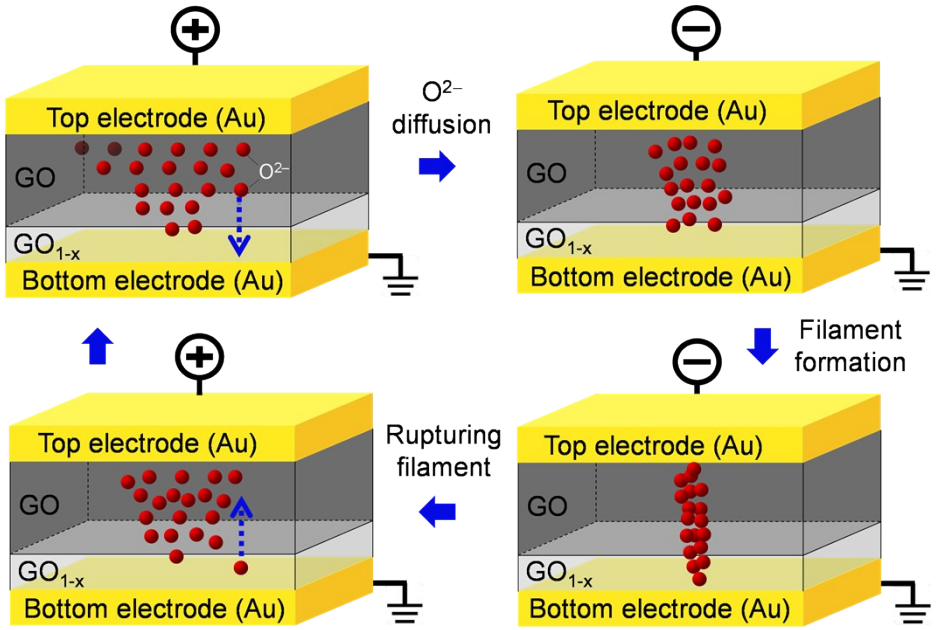

Supplementary Figure 4. Proposed mechanism. Schematic of the proposed mechanism of POG-graphene RRAMs.

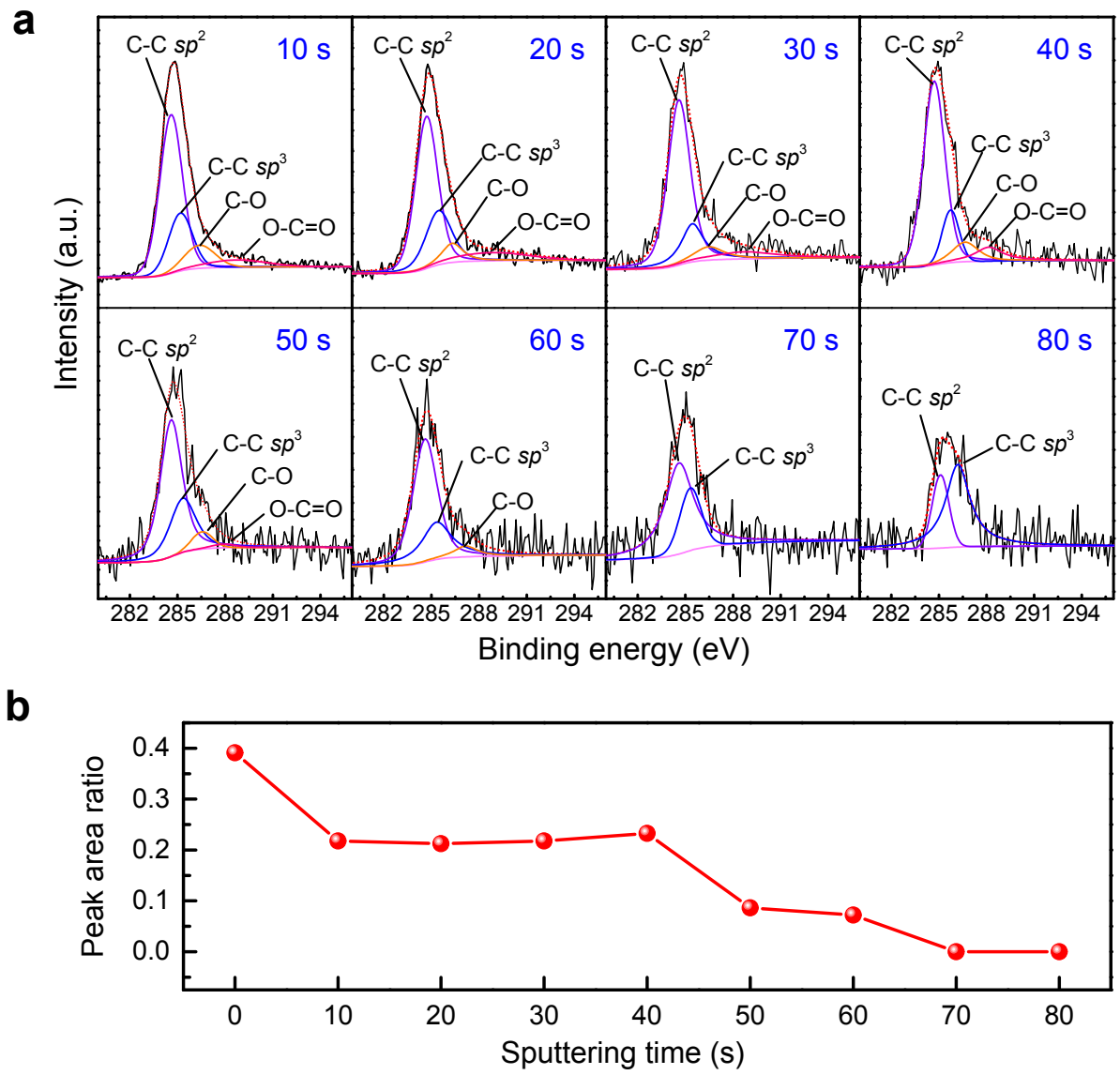

Supplementary Figure 5. XPS depth profile of POG-graphene. (a) XPS spectra of POG-graphene after etching for different durations. (b) Area ratio of carbon-oxygen peaks (C-O and O-C=O) relative to carbon peaks (C-C sp^2 and C-C sp^3) as a function of sputtering time.

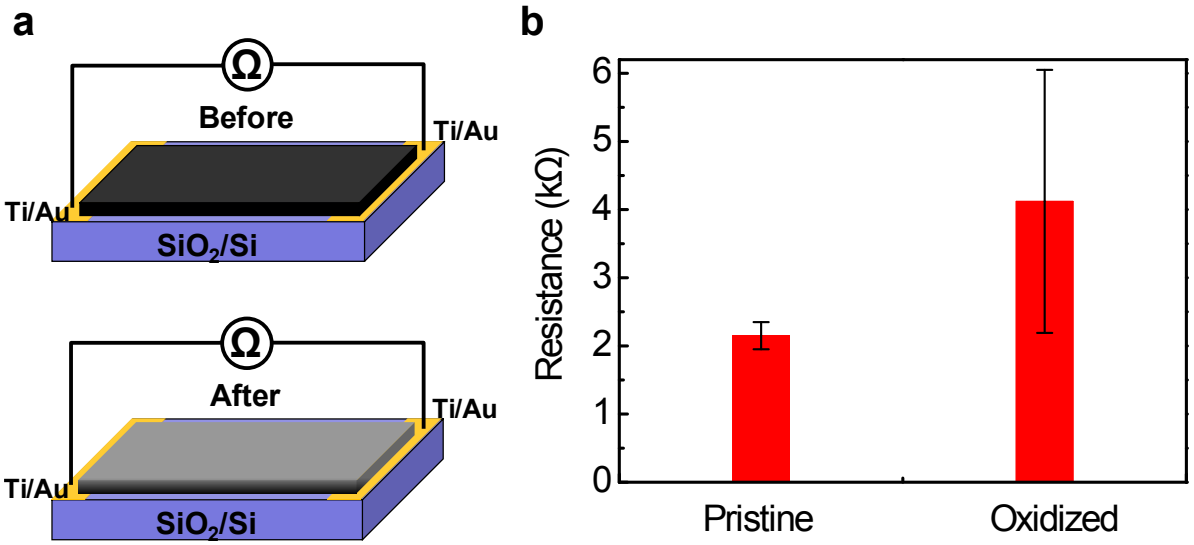

Supplementary Figure 6. Lateral resistance change of graphene films before and after the single-side ozone oxidation. (a) Schematics of the two-electrode device for resistance measurement from the bottom side. (b) Lateral resistance change of the 7-layer graphene film before and after single-side ozone treatment. The resistance of graphene film increases 1.9 times after oxidation without completely forming insulating graphene oxide. This result suggests that oxygen mainly penetrates and oxidizes the top layers, and the concentration of oxygen drops gradually to a negligible level for the bottom layers.

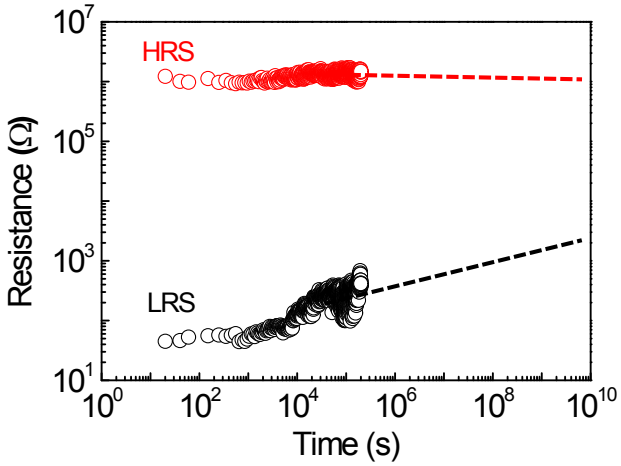

Supplementary Figure 7. Lifetime of the POG-graphene RRAMs. Extrapolated retention is estimated to be beyond 10 years.

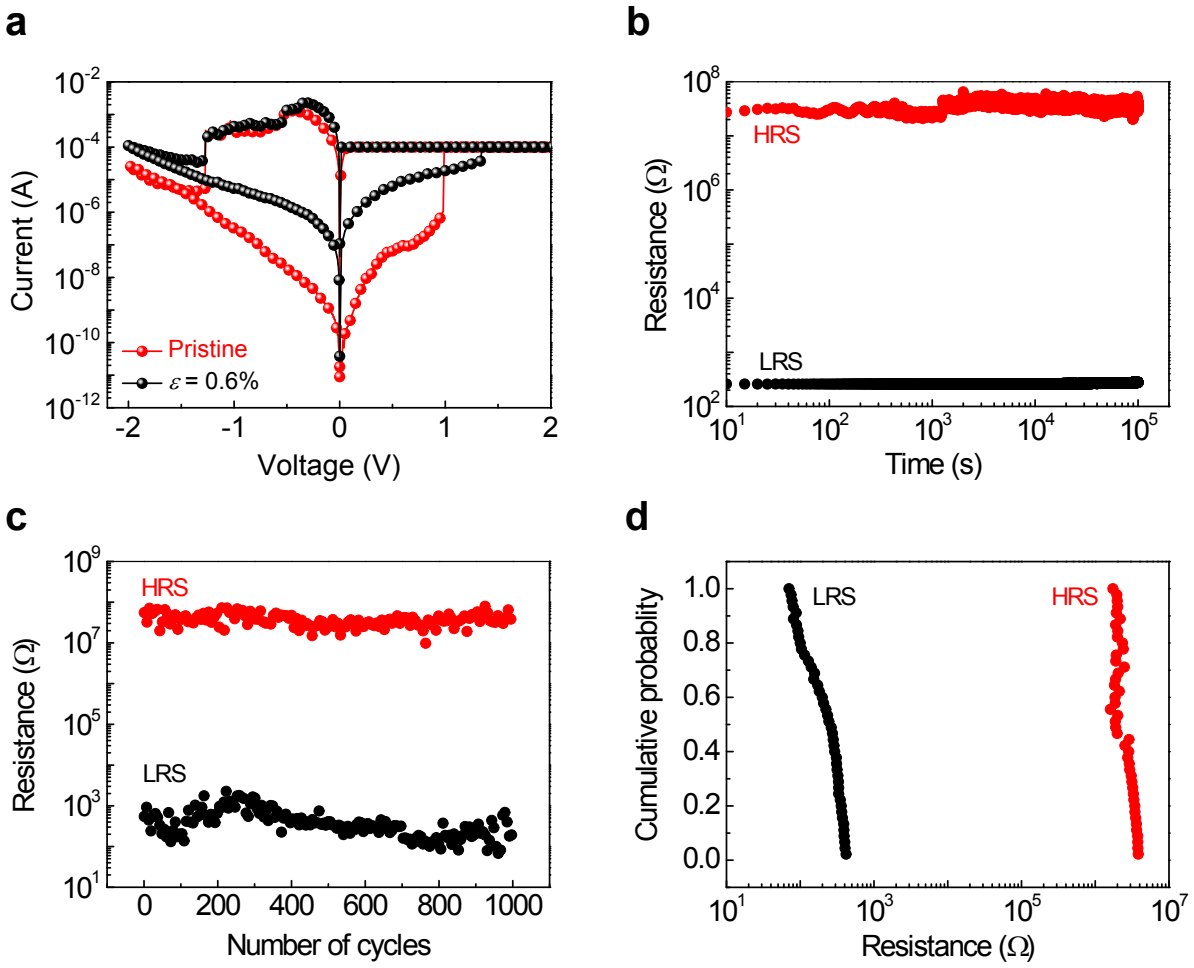

Supplementary Figure 8. Evaluation of the electrical performance of the POG-graphene RRAMs on a PEN substrate. (a) *I-V* characteristics of an individual RRAM in the pristine state and with 0.6% bending strain. (b) Retention and (c) endurance characteristics of the POG-graphene RRAMs obtained in the LRS and HRS at a constant read voltage of 0.1 V. (d) Device-to-device cumulative probability of the LRS and the HRS.

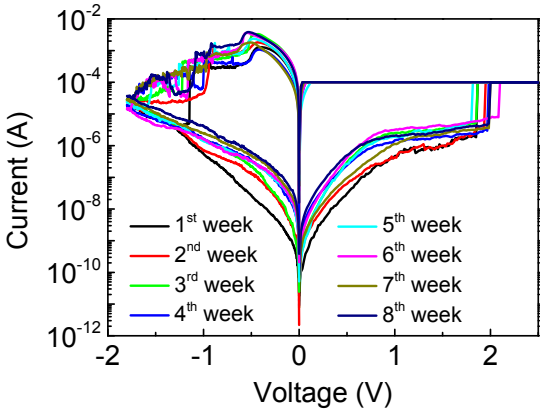

Supplementary Figure 9. Device reliability. *I-V* characteristics of a POG-graphene RRAM measured for eight weeks.

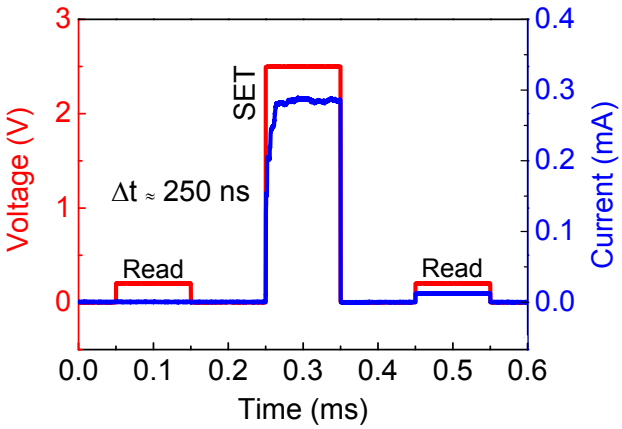

Supplementary Figure 10. Device operation speed. SET speed of a POG-graphene RRAM is about 250 ns under 2.5 V/100 μs sequential bias pulses.

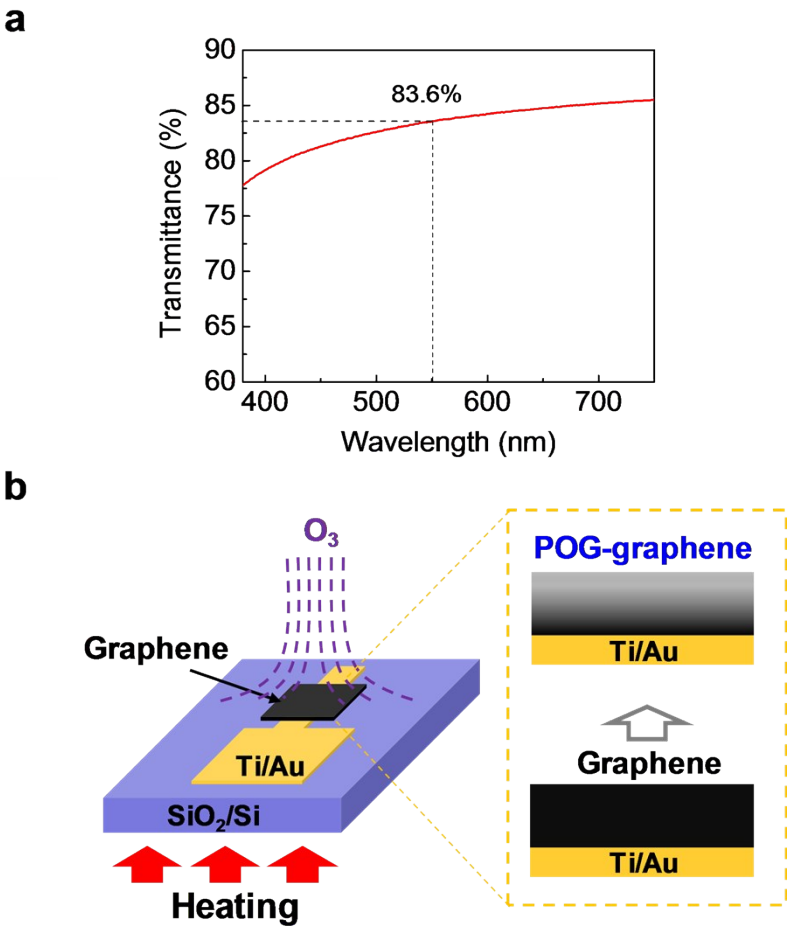

Supplementary Figure 11. Preparation of POG-graphene. (a) Optical transmittance spectrum of the 7-layer graphene film synthesized by metal-catalyst-free CVD. (b) Controllable single-side ozone oxidation of the 7-layer graphene to prepare the POG-graphene film.